Bulletin of the Seismological Society of America, Vol. 92, No. 8, pp. 3116–3133, December 2002

Comparison of Shear-Wave Slowness Profiles at 10 Strong-Motion Sites from Noninvasive SASW Measurements and Measurements Made in Boreholes

by Leo T. Brown,* David M. Boore, and Kenneth H. Stokoe II

Abstract The spectral-analysis-of-surface-waves (SASW) method is a relatively new *in situ* method for determining shear-wave slownesses. All measurements are made on the ground surface, making it much less costly than methods that require boreholes. The SASW method uses a number of active sources (ranging from a commercial Vibroseis truck to a small handheld hammer for the study conducted here) and different receiver spacings to map a curve of apparent phase velocity versus frequency. With the simplifying assumption that the phase velocities correspond to fundamental mode surface waves, forward modeling yields an estimate of the subsurface shear-wave slownesses.

To establish the reliability of this indirect technique, we conducted a blind evaluation of the SASW method. SASW testing was performed at 10 strong-motion stations at which borehole seismic measurements were previously or subsequently made; if previously made, the borehole results were not used for the interpretation of the SASW data, and vice-versa.

Comparisons of the shear-wave slownesses from the SASW and borehole measurements are generally very good. The differences in predicted ground-motion amplifications are less than about 15% for most frequencies. In addition, both methods gave the same NEHRP site classification for seven of the sites. For the other three sites the average velocities from the downhole measurements were only 5–13 m/sec larger than the velocity defining the class C/D boundary. This study demonstrates that in many situations the SASW method can provide subsurface information suitable for site response predictions.

Introduction

In situ shear-wave slowness profiles are used in a variety of earthquake engineering applications, including site response studies, liquefaction analyses, and soil–structure interaction evaluations. Borehole seismic methods such as the crosshole and downhole methods traditionally have been employed to measure shear-wave slowness (slowness is simply the reciprocal of velocity) in the field, since they are direct measurements. More recently, a suspension logger (made by the Oyo Corporation) has been used for this purpose, particularly in boreholes with depths of 100 m and more (the data from this instrument is referred to here as a PS log). Until now, seismic surface-wave methods, involving either Love or Rayleigh waves, have received little attention. Surface-wave methods involve more assumptions, unknowns, and numerical simulations than borehole methods. Surface-wave methods, however, offer the advantage of being noninvasive; hence, they are less costly and more rapidly conducted than borehole methods. A number of studies have inverted surface-wave phase velocities, obtained from both passive and active sources, to derive near-surface material properties (e.g., Horike, 1985; Zywicki, 1999); in this study we use a particular method known as the spectral-analysis-of-surface-waves (SASW) method (Stokoe *et al.*, 1994). The reliability of the SASW method needs to be established for it to gain widespread use in earthquake engineering.

Following the 1994 Northridge, California, earthquake, the U.S. Geological Survey drilled a number of boreholes at sites from which recordings of the ground motion were obtained (Gibbs *et al.*, 1999). Several of the authors realized that this presented an excellent opportunity to test the SASW method at borehole sites. SASW measurements at a number of these sites were made in the summer of 1997, and inter-

*Present address: Phillips Petroleum, 680-B Plaza Office Building, Bartlesville, Oklahoma 74004; e-mail: *ltbrown@ppco.com*.

pretation of the measurements was done in a truly blind manner, using no information from the downhole measurements. These results are contained in the Master's thesis of the first author (Brown, 1998). While preparing those results for publication, it was discovered that Brown (1998) used the common assumption that Poisson's ratio was 0.25 in his modeling of the observed dispersion. Although a good assumption for most of the Earth, as shown in Figure 1, it is a poor assumption for near-surface soil that is saturated. This is so because the compressional wave velocity is controlled by the velocity of water (around 1500 m/sec) and is not well correlated with shear-wave velocity, and as a result, Poisson's ratio can approach 0.5 in the saturated materials. The assumption of 0.25 for Poisson's ratio produces *P*-wave slownesses that are too high below the water table, and fitting the dispersion data then leads to *S*-wave slownesses that in general are systematically low. Because of the anticipated systematic changes in the derived slownesses, we decided to reinterpret the data. To preserve the blind nature of the study, the files containing the dispersion curves were assigned nonsensical names by the second author (D.M.B.) and sent to the first author (L.T.B.), who derived the slowness models from these randomly named files without use of previous results or site information. The approximate water-table depth was given to L.T.B. by D.M.B., since this information is generally available from a geologic investigation or could be obtained from a *P*-wave refraction survey (the term "water table" is loosely used here to represent the top of the saturated zone). In the modeling, Poisson's ratio was assumed equal to 0.33 above the water table; below the water table Poisson's ratio was calculated using a compressional velocity equal to 1500 m/sec or with Poisson's ratio equal to 0.25, if greater.

In this article we compare results from the SASW method and borehole measurements (both downhole logs and PS logs, if available) at 10 sites. These sites are shown in Figure 2, with additional information contained in Table 1. We first give an overview of the borehole and the SASW methods. This is followed by a presentation of results at two sites for which the comparisons were good and not so good (but for a known reason). Finally, we compare results for all 10 sites. We find that overall the SASW results compare favorably with the borehole results. The favorable comparison differs from that found in a previous article (Boore and Brown, 1998a,b). The earlier article compared shear-wave velocities from borehole results and a specific application of a by-now outdated noninvasive procedure, and the conclusions were intended to warn users that the results of that application might contain biases. Our earlier article contained no conclusions regarding other noninvasive methods, although we fear that a number of readers misinterpreted our results to indicate that in general surface-wave methods

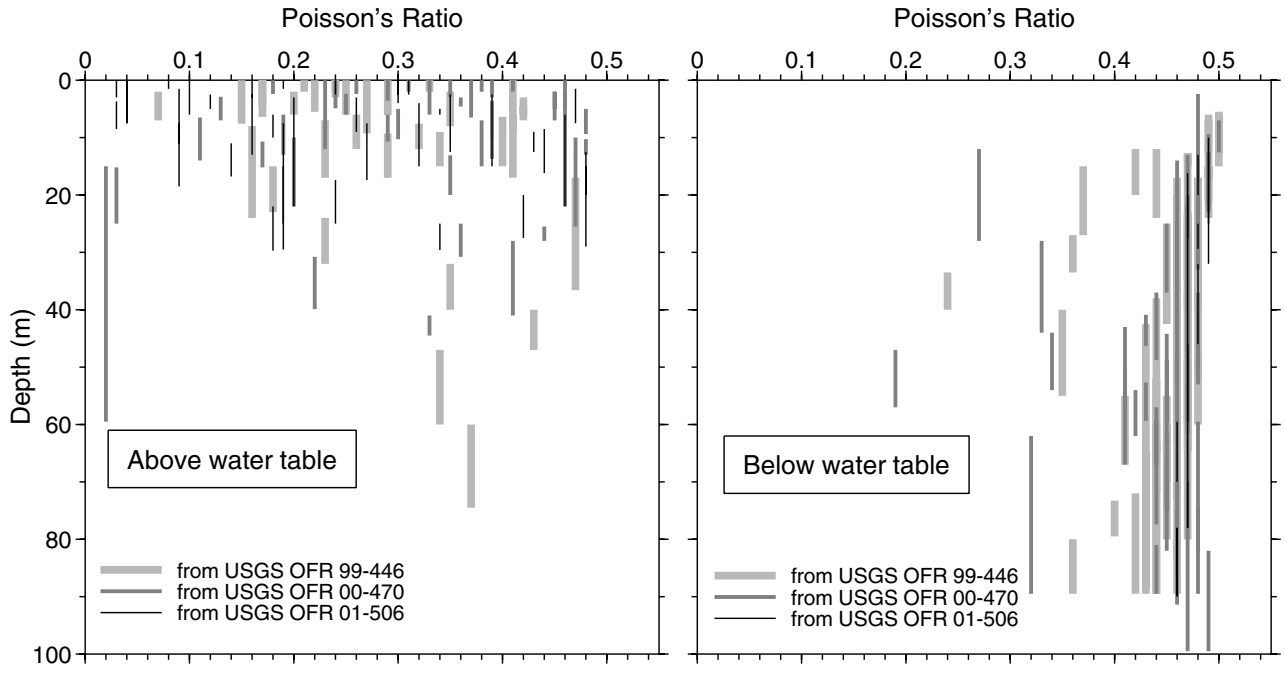

Figure 1. Poisson's ratio versus depth for material above and below the water table, using values from recent measurements of velocities in southern California (Gibbs *et al.* 1999, 2000, 2001). The length of each vertical line spans the depth range for each particular constant-velocity layer from which Poisson's ratio was determined. All except one of the few values in the righthand plot, for which Poisson's ratio is less than 0.4, correspond to cases for which the *S* velocity is high (i.e., rock, where the *P* velocity is not controlled by water velocity). The one exception is a "dry" layer below the water table (with low *P* velocity).

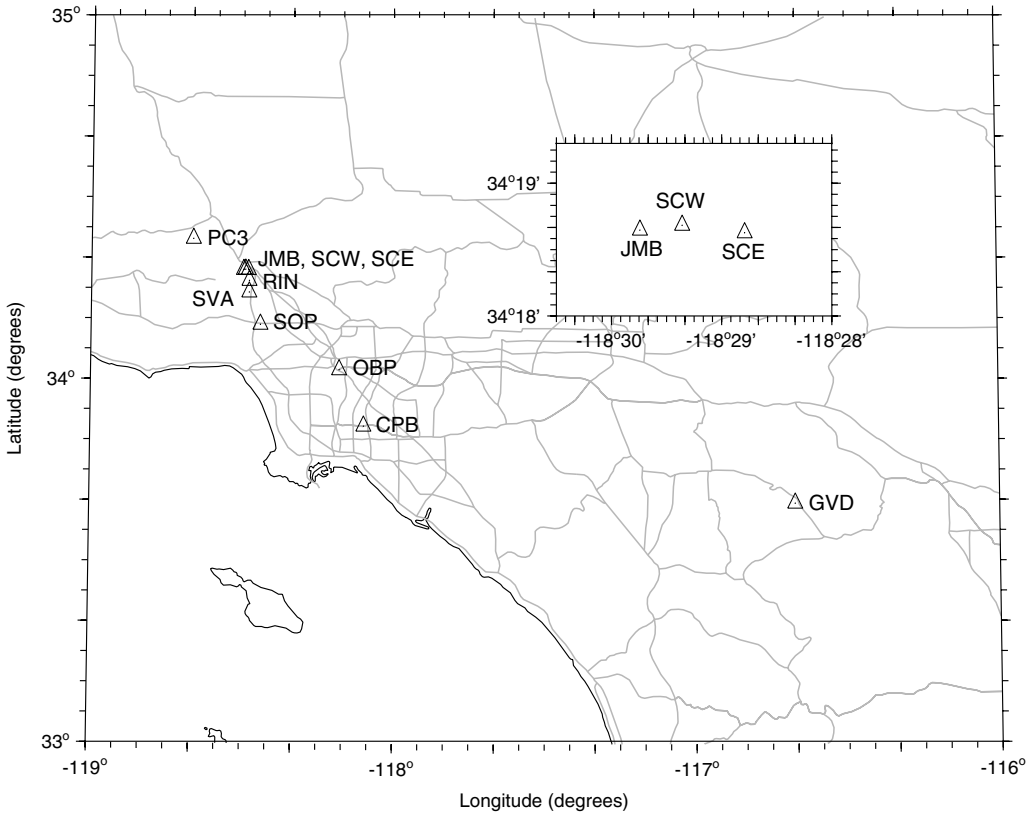

Figure 2. Site map of Los Angeles region showing the locations of SASW testing sites in this study. The gray lines show the major roads, and the inset shows the relative locations of boreholes JMB, SCW, and SCE.

might produce biased results. We hope that the current article dispels this erroneous conclusion.

Why Slowness Rather Than Velocity?

Before getting into the heart of the article, we feel it important to discuss a departure we have made from the traditional use of shear-wave velocity as the material property of interest. The fundamental material property used in this article is the shear-wave slowness. This is nothing more than the reciprocal of shear-wave velocity. Why introduce and use an unfamiliar quantity? There are several reasons. First, it is a more fundamental quantity than the velocity for site response studies. Theoretical responses of layered systems, both site response and surface-wave dispersion, involve travel time across the layers, and this travel time is linearly proportional to the slowness ($t = s \times h$, rather than $t = (1/v) \times h$, where t is travel time, s is slowness, v is velocity, and h is layer thickness). Second, slowness models from a number of boreholes can be averaged directly depth by depth to obtain an average slowness profile for a certain class of sites (linear averaging of velocities, as is sometimes done, is incorrect). Third, interpretations of travel times from borehole measurements usually involve fitting lines to travel time versus depth; the slope of this fit is slowness, not velocity, and the statistics of the fit apply to slowness rather than velocity. Fourth, and probably most important for this study, a visual comparison of slowness versus depth obtained from different methods (such as the SASW and the downhole methods discussed here) is preferable to comparing velocities: apparent large differences in velocities in the deeper, higher velocity portions of a profile attract the eye but are less important in site response than less pronounced differences in the lower velocities near the surface—plotting slowness emphasizes differences in material properties of most importance for site response (which is again fundamentally related to the time a wave spends in a layer). Because of the unfamiliarity of slowness, all figures involving slowness in the text are repeated using velocity in the Appendix.

Overview of Downhole Seismic and *PS* Suspension Logging Data

The downhole seismic method (more accurately called the surface-source, downhole receiver method) is described by Gibbs *et al.* (1999). Surface sources for *P* and *S* waves are used to propagate elastic waves downward to an in-hole receiver, which is moved down the hole, thus providing a record section of waveforms for a series of depths. First

Table 1
Borehole Information

Borehole Name	Code	Lat. (°)	Long. (°)	Distance (m)		V_{30} (m/sec)		Class	
				CL	CD	DH	SASW	DH	SASW
Cerritos College: Police Building	CPB	33.88212	−118.0968	76	2	250	234	D	D
Garner Valley Downhole Array	GVD	33.6688	−116.673	5	5	282	275	D	D
Jensen Filtr. Plant: Admin. Bldg	JMB	34.3111	−118.4957	76	18	373	298	C	D
Obregon Park	OBP	34.03699	−118.17781	205	198	349	300	D	D
Potrero Canyon: Borehole 3	PC3	34.39522	−118.66317	4	4	205	246	D	D
Rinaldi Receiving Station	RIN	34.281	−118.4771	62	3	333	321	D	D
Sylmar Converter Station East	SCE	34.31077	−118.47986	72	6	370	323	C	D
Sylmar Converter Station West	SCW	34.3117	−118.4893	23	20	251	260	D	D
Sherman Oaks Park	SOP	34.1607	−118.4394	35	19	301	270	D	D
Sepulveda V. A. Hospital	SVA	34.249	−118.4772	52	50	365	285	C	D

CL and CD are the distances from the borehole to the centerline and to the point of closest approach of the SASW linear array; Class is the NEHRP site class, defined by V_{30}.

arrivals are fit using a least-squares procedure with a model consisting of constant velocity, laterally uniform layers. The refraction of the rays between layers is taken into account in the analysis. In a sense, the model represents material properties averaged laterally from the borehole over a distance of a fraction of a wavelength (10 m is a typical wavelength for *S* waves in soils at the frequencies produced by the *S*-wave source). Additionally, as with all wave-arrival methods, the stiffest materials in the borehole vicinity are measured.

The PS suspension logging method is described by Nigbor and Imai (1994). A probe with a seismic source and two receivers is used to make interval *P*- and *S*-wave arrivals for a series of borehole depths, from which slowness or velocity can be computed. High resolution data can be obtained (every 0.5 m) with no decrease in resolution with depth. Data quality depends on borehole conditions. The best results are obtained for an uncased borehole. On the other hand, the downhole logging method requires cased holes (in order to clamp the receiver at various depths), and therefore all holes discussed in this article were cased. Fortunately, casing of the holes drilled for the downhole logging was usually postponed until the day after the drilling was completed. This allowed time for PS logging in the evening after the holes were drilled, but before they were cased.

Overview of SASW Method

Spectral-analysis-of-surface-waves (SASW) testing, initially developed at the University of Texas at Austin, is an *in situ* seismic method for determining shear-wave velocity or slowness profiles (Stokoe *et al.*, 1989, 1994; Nazarian and Stokoe, 1984). It is noninvasive and nondestructive, with all testing performed on the ground surface at strain levels in the soil in the elastic range (shear strains $< 0.001\%$). A detailed description of the SASW field procedure is given in Brown (1998) and Joh (1997). A vertical dynamic load is used as the source of the waves. For this investigation, a Vibroseis truck, commonly used for seismic exploration in the oil industry, was used to generate the long wavelengths. Various handheld hammers were used for the short wavelengths. The ground motions were monitored by two vertical receivers (70% critically damped 1-Hz geophones) and recorded by a dynamic signal analyzer. A schematic of this is shown in Figure 3. To minimize phase shifts due to differences in receiver coupling and subsurface variability, the source location was reversed. Theoretical as well as practical considerations, such as attenuation, necessitated the use of several receiver spacings (generally keeping the same centerpoint for the array) to generate the dispersion curve over the wavelength range required to evaluate the stiffness profile to a depth of 100 m. Typical interreceiver spacings were 1.8, 3.6, 7.6, 15.2, 30.5, 61, and 122 m. The distance from the source to the first receiver was nominally the same as the interreceiver distance.

The phase differences between the two receivers, obtained in the frequency domain from the dynamic signal analyzer, were processed to unwrap the phase and remove noisy or incoherent portions. These phase differences were converted to apparent phase velocities using the equation

$$V_R = 2\pi f d_2/\Delta\phi, \quad (1)$$

where f is the frequency, d_2 is the distance between receivers (Fig. 3), and $\Delta\phi$ is the phase difference in radians. Each source and receiver combination produced one set of apparent velocities. Because there are a number of source and receiver combinations in the measurements done at any one site, there are typically several thousand data points. For a particular source-receiver combination, the dispersion data are limited to wavelengths less than one half of the distance from the source to the first receiver in an attempt to minimize the distortion due to near-source effects and body waves. For interpretation, an average curve of V_R versus frequency was computed. This curve is referred to as a "compact dispersion curve." Note the use of the term "dispersion curve." The basic data are phase differences, which can be produced by any complicated set of waves. Because of the surface

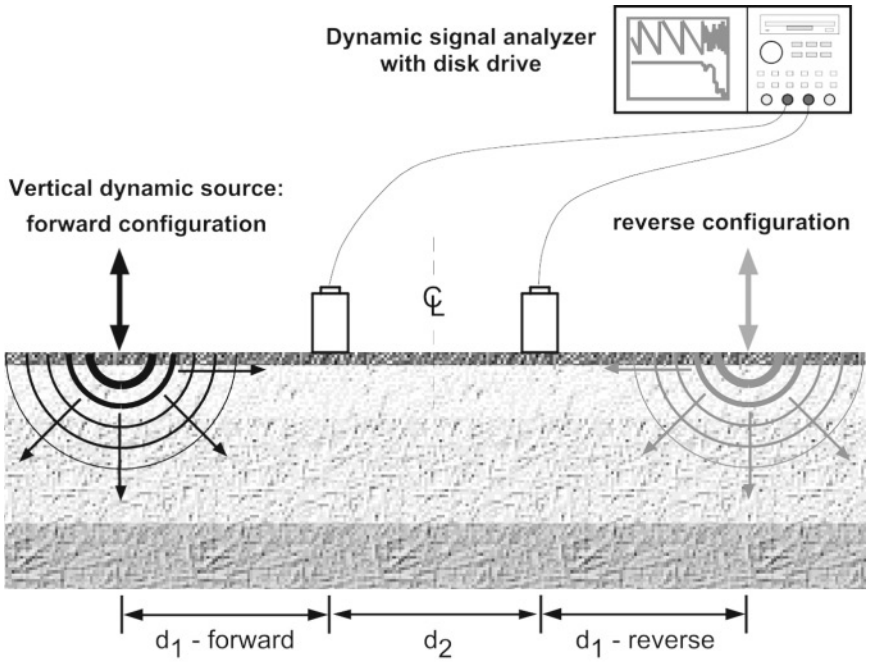

Figure 3. Basic configuration of SASW measurements (modified from Joh, 1997).

source and the source-receiver spacings used in the method, the phase differences are usually controlled largely by fundamental mode surface waves, in which case the curve of apparent velocity versus frequency is a dispersion curve. The analysis method we employed assumes that the phase differences are solely due to fundamental mode Rayleigh waves. More complicated analyses can be performed in which the complete wavefield is modeled; in view of the good results we obtained, however, we felt that the significant increase in complexity to do this was not warranted. In addition, doing only the simple analysis is also in keeping with the spirit of this article—seeing how well the most straightforward application of the SASW method does in comparison to borehole results.

The analysis of the SASW data was performed using the program WinSASW, a program developed at the University of Texas at Austin to reduce and interpret the dispersion curve (Joh, 1992). Through iterative forward modeling, a shear-wave slowness profile was found whose theoretical dispersion curve is a close fit to the field data. The final model profile is assumed to represent actual site conditions, and it represents an average laterally over a distance comparable to the SASW array (ranging from less than a meter at high frequencies to 200 m or so at low frequencies).

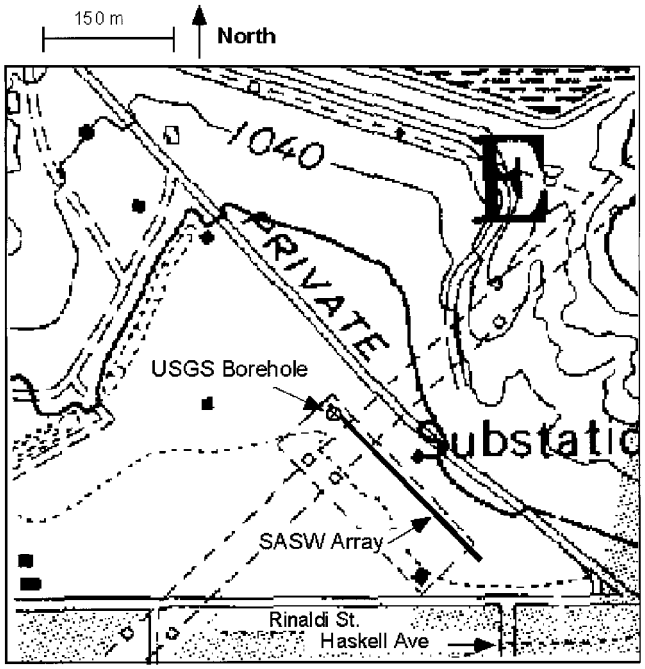

Figure 4. Site map for Rinaldi Receiving Station, showing approximate testing locations.

Procedure

The SASW method, described previously, was used to collect surface-wave dispersion data at each of the 10 sites shown in Figure 2 (site information is contained in Table 1). The linear arrays required by the SASW method were placed as close as possible to the boreholes, with distances ranging from 4 to 205 m from the borehole to the center of the array (Table 1).

Comparisons of borehole and SASW results were made in two ways: plots of slowness versus depth, and plots of ratios of amplification versus frequency. The reasons for comparing slowness rather than velocity were discussed ear-

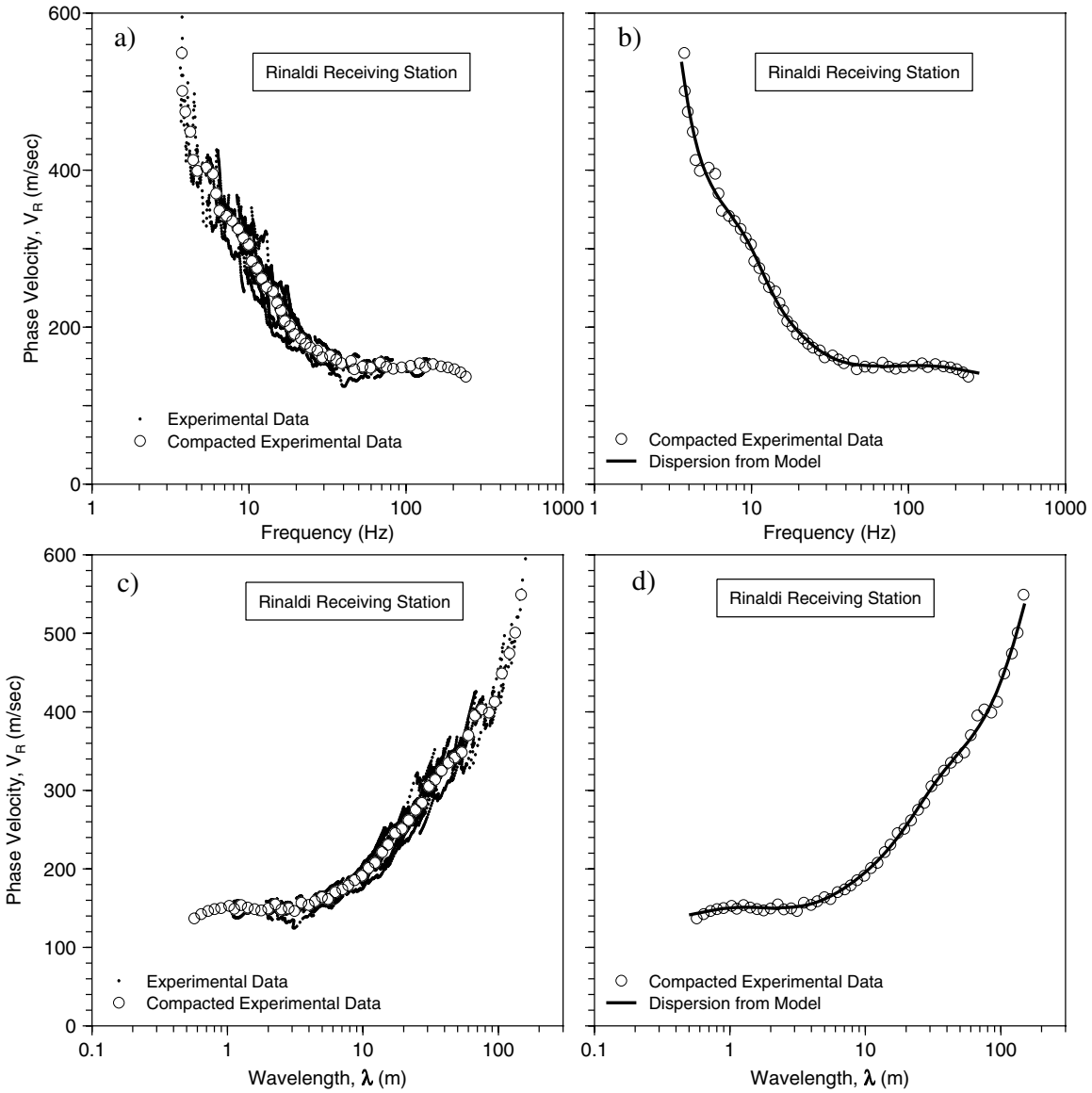

Figure 5. Dispersion measured at Rinaldi Receiver Station displayed using different abscissas (frequency in graphs in the first row and wavelength in the second row). The graphs in the first column compare the composite experimental and compacted dispersion curves, whereas the graphs in the second column show the fit between compacted experimental and theoretical dispersion curves.

lier. In this section we discuss the method used to compute the ratio of amplifications.

An important use of the subsurface properties obtained from either borehole or SASW studies is in estimating site response of earthquakes. For this reason it is reasonable to compare the consequences of different profiles on ground-motion amplification at the same site. This could be done in the usual way by computing the response of the layered models to incident *SH* waves, using matrix methods that incorporate all reverberations, and then forming the ratio of these responses. Although easy to do, each site response will contain peaks and valleys due to the complex interaction of the reverberating waves, and the ratio of these amplifications can be dominated by these peaks and valleys. Each profile, however, has some uncertainty, and this uncertainty will produce shifts in the precise frequencies at which these peaks and valleys occur; these shifts can significantly alter the appearance of a ratio of site amplifications. For this reason we have adopted a smooth estimate of amplification that averages out the peaks and valleys. These amplifications are based on the square root of the seismic impedance ratio, where the seismic impedances are frequency dependent, being obtained using velocities averaged over depths corresponding to a quarter wavelength (see, e.g., Boore and Joyner, 1997; Boore and Brown, 1998a,b; and Boore, 2003). Assuming vertically propagating shear waves and the same

density profile for the different slowness profiles, the ratio of the amplifications reduces to

$$A_{\mathrm{SASW}}(f)/A_{\mathrm{DH}}(f) = \sqrt{\bar{S}_{\mathrm{SASW}}(f)/\bar{S}_{\mathrm{DH}}(f)}, \qquad (2)$$

where $A(f)$ is the square-root impedance ratio amplification approximation for SASW or downhole (DH) slowness profiles, as indicated by the subscript. The fundamental quantity in the calculations is the travel time, tt, from the surface to a given depth, z, given by:

$$\mathrm{tt}(z) = \sum S_i h_i, \qquad (3)$$

where h_i is layer thickness and S_i is the layer shear-wave slowness. The average slowness $\bar{S}$ to depth z is given by

$$\bar{S} = \mathrm{tt}(z)/z, \qquad (4)$$

and the frequencies are determined by the first mode of vibration of a system composed of a layer of thickness z and constant slowness equal to $\bar{S}$ over a half-space:

$$f(z) = 1/[4\mathrm{tt}(z)]. \qquad (5)$$

In equation (2) the ratio of average slownesses is for the same frequency, but because the profiles differ, for a given frequency the averages are for different depths.

SASW Testing Results at Two Example Sites

Two sites were chosen to illustrate the details of the experimental procedure and the method of comparison. The two sites were chosen because they are examples of good and poor comparisons of results. The two sites are the Rinaldi Receiving Station (RIN) and the Sepulveda Veterans Administration Hospital (SVA).

The location of the SASW array and the borehole at Rinaldi Receiving Station are shown in Figure 4. Based on surficial geology, little variation in near-surface material is expected over the dimension of the SASW array. The experimental data and compact dispersion curve are shown in Figure 5. (The expectation of little lateral variability is confirmed in Figures 5a and 5c by the continuity in the dispersion curves for the seven receiver spacings.) The results are displayed using both wavelength and frequency as the abscissa. Frequency is a true independent variable, but wavelength is a more physically meaningful quantity. The compact dispersion curve is well defined by the individual data points. Also shown in Figure 5 is the comparison between the compact dispersion curve and the theoretical fundamental-mode Rayleigh-wave dispersion curve for the final model obtained in the iterative modeling procedure. The fit between the theoretical and observed dispersion is excellent. A comparison of slowness obtained from borehole studies and the SASW method is given in Figure 6. Qualitatively, the comparisons are quite good; as shown subse-

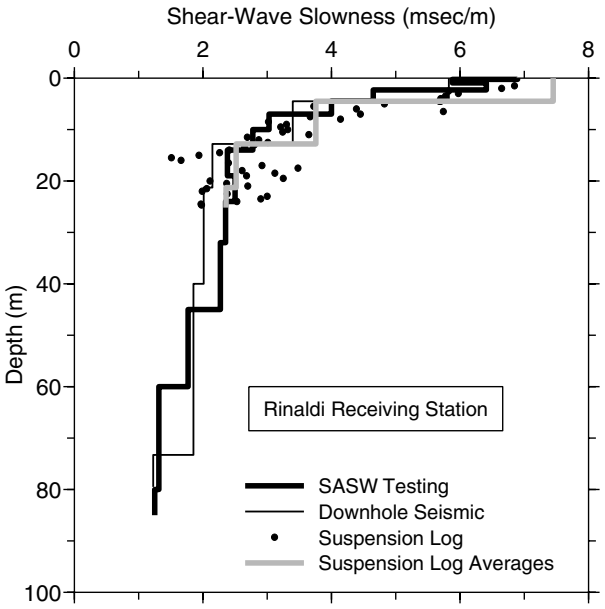

Figure 6. Comparison of shear-wave slownesses for Rinaldi Receiving Station, derived from the SASW, downhole, and PS log methods. Also shown are the averages of the PS results over depth intervals equal to the downhole model (the two shallowest PS values, between 10 and 12 msec/m, are off the scale of the plot, which explains why the average for the shallowest layer seems to be greater than the individual PS values).

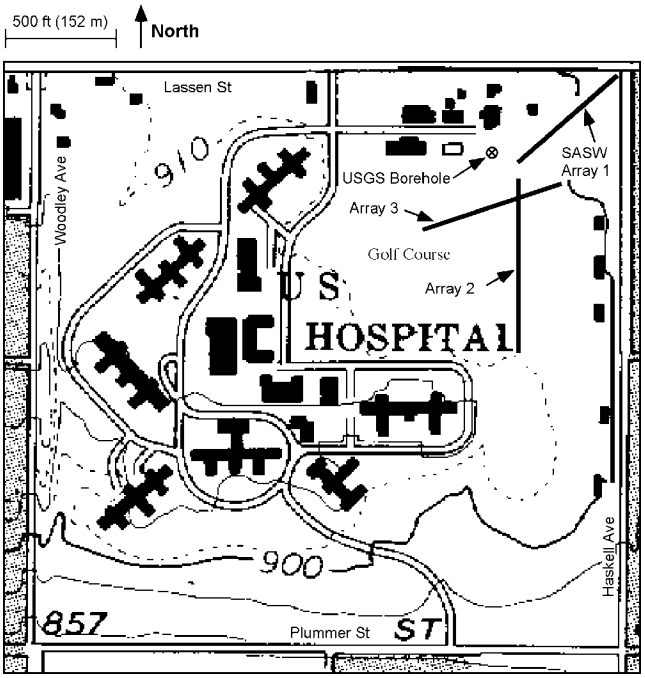

Figure 7. Site map for SVA Hospital, showing approximate testing locations.

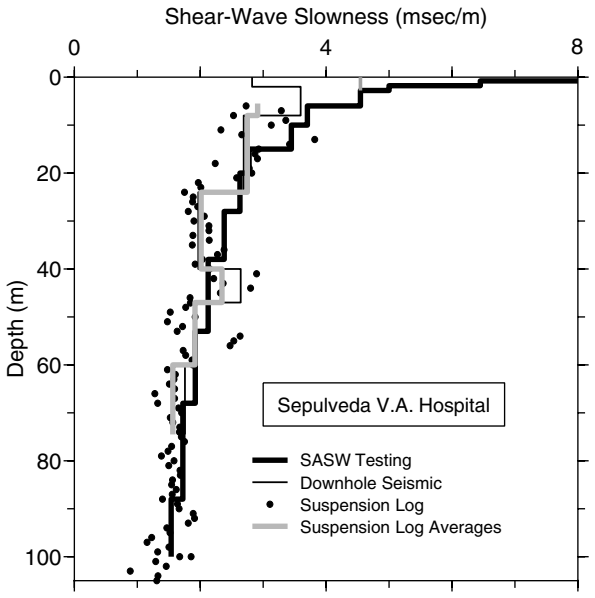

Figure 8. Comparison of shear-wave slownesses for SVA Hospital, derived from the SASW, downhole, and PS log methods. Also shown are the averages of the PS results over depth intervals equal to the downhole model. The two shallowest SASW values, 8.3 msec/m and 11.1 msec/m, are off the scale of the plot. As discussed in the text, a model in which the SASW slowness is capped at 4.55 msec/m was considered in the site response calculations; the alteration near the surface for this model is shown by the short gray line.

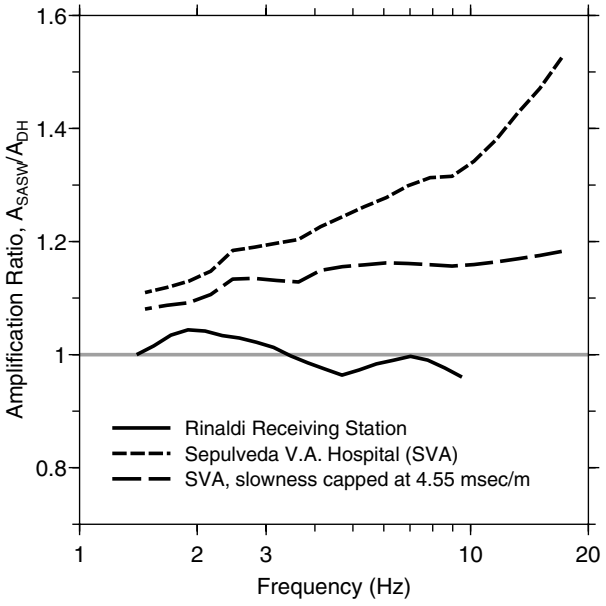

Figure 9. Amplification ratios (from SASW and downhole slownesses) versus frequency, assuming a square root impedance approximation for earthquake site response, for Rinaldi Receiving Station and SVA Hospital (using slownesses as measured and as capped at 4.55 msec/sec). The USGS downhole profile is the reference profile.

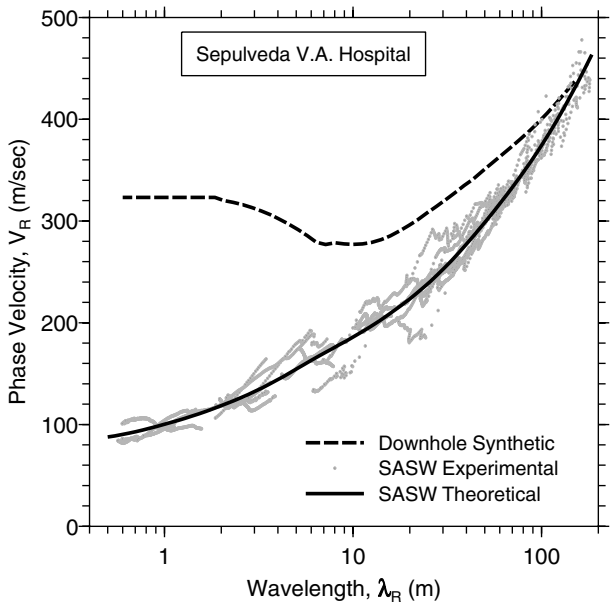

Figure 10. Comparison of theoretical (synthetic) dispersion curve based on the downhole velocity profiles with the experimental dispersion curve from SASW measurements. The effect of differences in near-surface velocities is shown clearly. Also shown is the fit of the theoretical dispersion curve based on the model derived from the SASW measurements with those measurements.

quently, the corresponding ratio of amplifications differs from unity by less than about 5%.

The site map for the Sepulveda V.A. Hospital (SVA) is shown in Figure 7. Unlike RIN, the near-surface materials are expected to differ between the borehole and the SASW arrays: a layer of compacted fill occurs at the ground surface in the vicinity of the borehole (Gibbs *et al.*, 1999), but the SASW arrays were placed on a well-watered golf course. Data from all three SASW arrays were combined and modeled to obtain the slowness profile that is compared with downhole and suspension logging results in Figure 8. At depth the profiles are similar, but large differences in slowness occur near the surface (we believe these are largely due to the differences in near-surface material just noted). These slowness differences lead to significant differences in site amplification, as shown in Figure 9 (this figure also shows the ratio of amplifications for RIN). The slowness differences only occur in the upper 15 m, but they lead to differences in amplification over a frequency range of prime engineering concern. In an attempt to eliminate the large slownesses presumably due to the moist materials beneath the golf course (the downhole and suspension log values were from a borehole away from the golf course), amplifications were also computed for a model in which the SASW values have been capped at 4.55 msec/m, as shown in Figures 8 and 9. This reduces the ratio of the amplifications to less than about 1.15 for most frequencies.

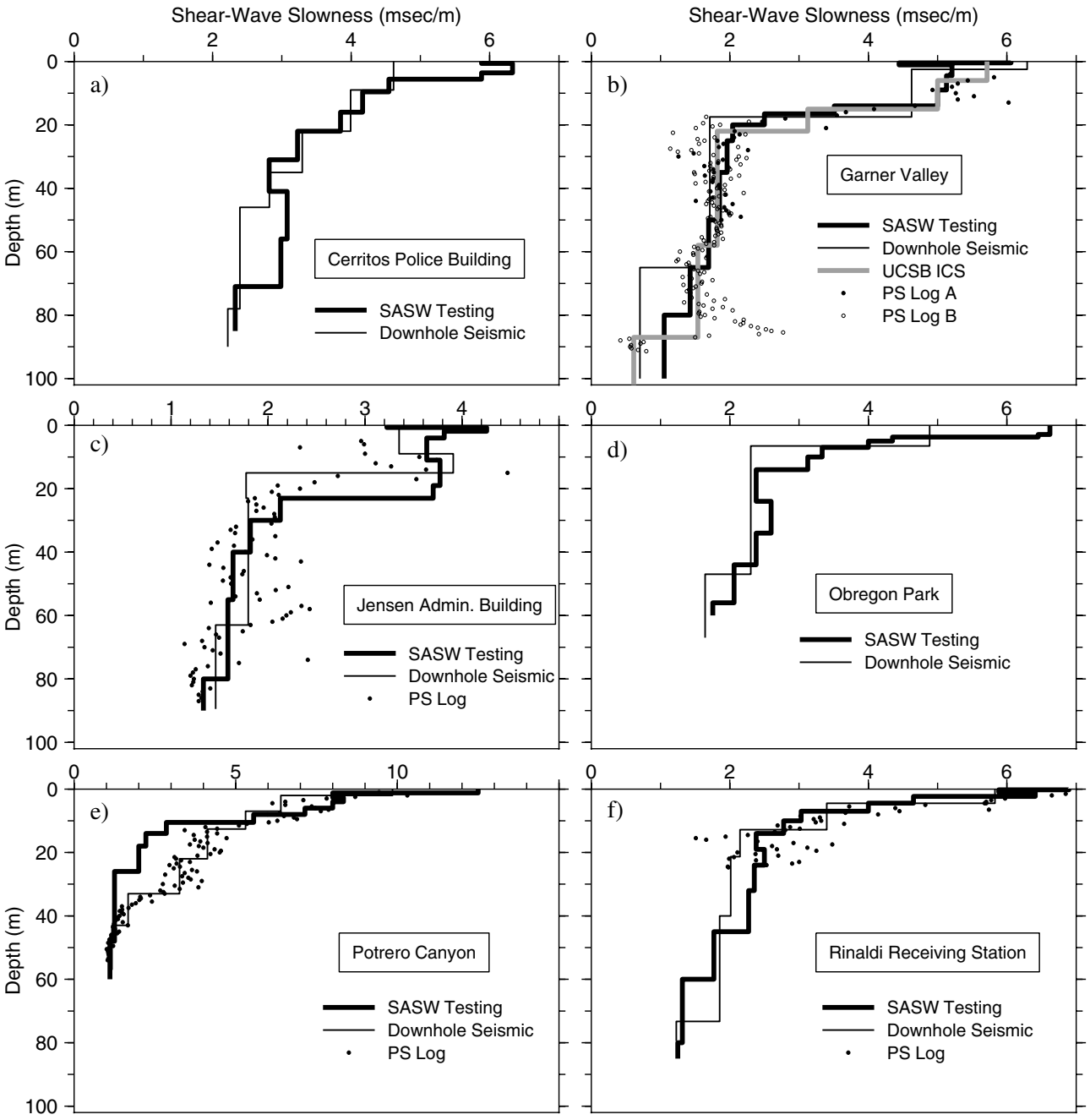

The differences in slowness are not due to uncertainty in the SASW model resulting from poor data. The observed data and the theoretical dispersion both for the SASW and the DH models are shown in Figure 10. The resolution of the SASW method is clearly capable of discerning the large differences in dispersion from the two models. We think that the models are good representations of the actual subsurface material beneath each measurement location and that there are significant lateral variations in the material properties in the upper 15 m.

Results

We summarize the comparisons for all 10 sites in Figures 11 (for slowness) and 12 (for amplification ratios). Sources of data are contained in the caption to Figure 11. Overall, the comparisons are quite good. There is a tendency for the SASW models to have a slightly larger slowness near the surface, which shows up as an amplification somewhat larger than predicted from the downhole models. But the difference is small (generally the ratios are less than about a factor of 1.15). Average velocities to 30 m and the corre-

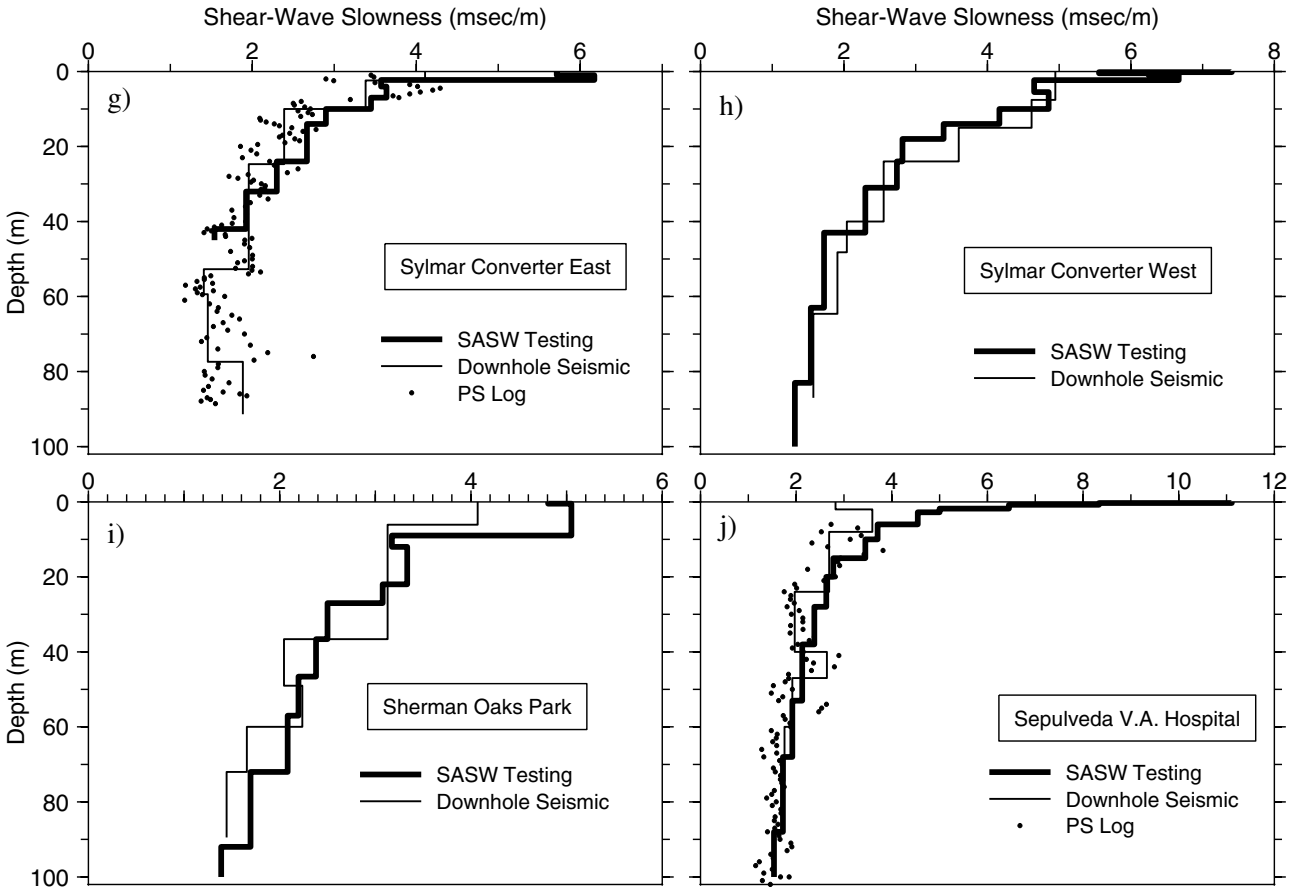

Figure 11. Shear-wave slownesses at all sites, derived from the SASW, downhole, and PS logging methods. Downhole models for Rinaldi Receiving Station, Sepulveda VA Hospital, Sherman Oaks Park, Sylmar Converter West, and Jensen Administration Building) are from Gibbs *et al.* (1999); models for Potrero Canyon, Sylmar Converter East, and Obregon Park are from Gibbs *et al.* (2000); models for Garner Valley are from a revision by the second author of Gibbs (1989); and models for Cerritos College Police Building are from Gibbs *et al.* (2001). Suspension logging models from the Resolution of Site Response Issues from the Northridge Earthquake (ROSRINE) web site (*http://geoinfo.usc.edu/rosrine/*). The UCSB ICS model for Garner Valley was based on suspension logging results and is published in Steidl *et al.* (1998).

sponding NEHRP site classes are given in Table 1. The average velocities are quite similar, but because a few are close to the site class C-D boundary (360 m/sec), three out of the ten sites have differences in the NEHRP site classes. We think that this illustrates the problematical nature of site class definitions when the average velocities are close to a class boundary rather than a limitation with the average velocities determined from SASW models; histograms of average velocities for extensive datasets show no indication of the class boundaries (e.g., Boore and Joyner, 1997; Wills *et al.*, 2000).

Part of the difference between the slowness profiles from downhole and SASW testing is due to the different layer interfaces. Layer intervals for the downhole profile were selected based on observed travel times and the borehole lithology log, whereas no site information was used in the SASW analysis. Lateral variability may also contribute to differences in shear-wave slowness. The downhole profile is almost a point measurement of the subsurface properties, whereas the SASW method averages properties over horizontal distances related to the array length. In many geologic environments there may be significant changes in the subsurface properties over the lateral dimensions averaged in the SASW method (this is especially true in the very near-surface materials), and therefore the slowness profiles for the two methods, although different, might accurately reflect the subsurface properties. In addition, neither method accounts for anisotropy, and at some of the sites the waves being measured by the SASW method may contain phases other than the fundamental mode Rayleigh wave.

As discussed in the introduction, the initial analysis of the SASW data assumed a Poisson's ratio of 0.25, whereas the analysis used for this article made use of the depth to the

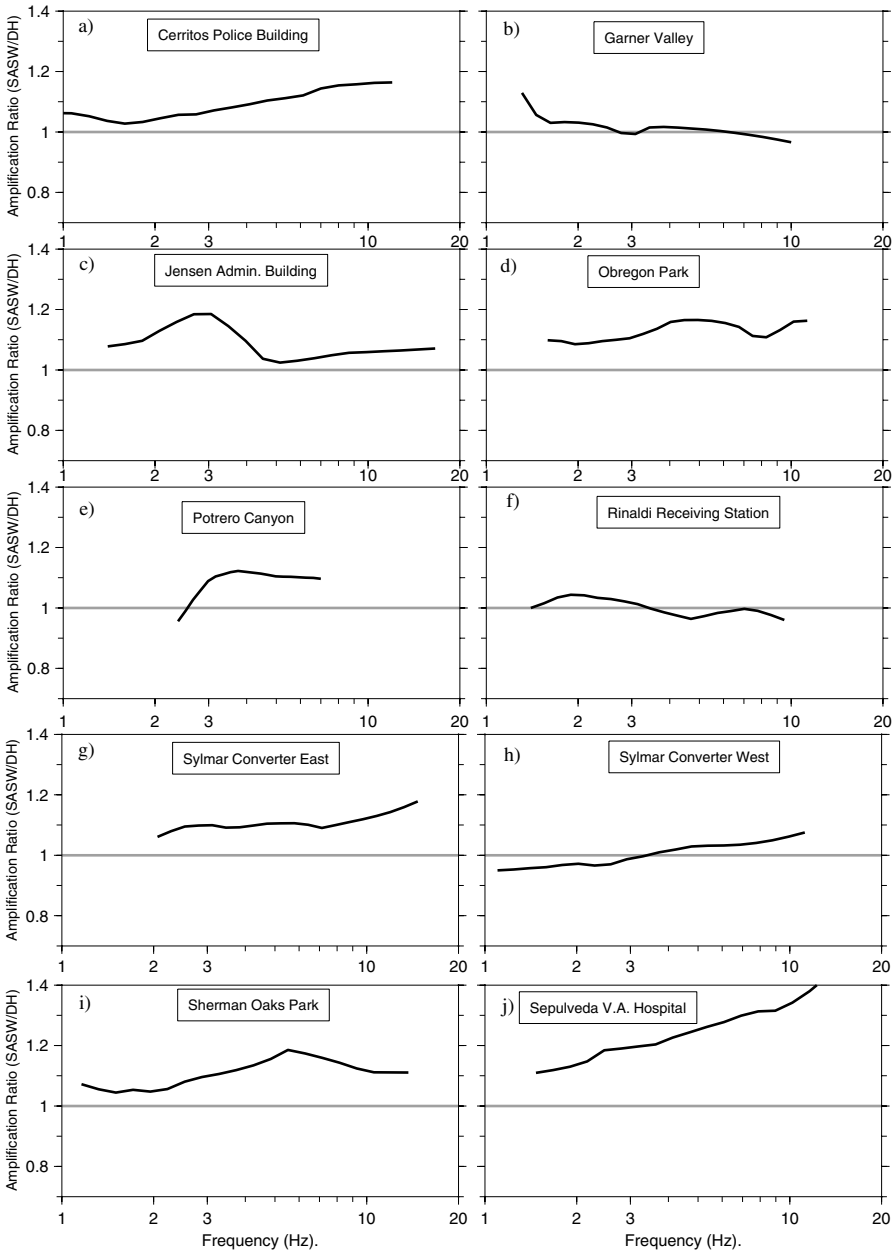

Figure 12. Ratio of square-root impedance amplifications from the SASW and downhole models for all sites.

water table. A comparison of slowness for the two sets of models is given in Figure 13. As expected, the largest differences are at depths below the water table, where the earlier assumption about Poisson's ratio is very poor. As a result of the change in Poisson's ratio, the slownesses of the *S* waves are generally higher (the velocities are lower) than in the initial analysis. This is a consequence of the assumption that the *P*-wave slownesses were overestimated in the initial analysis, leading to an underestimation of the *S*-wave slownesses as a compensation (recall that the same dispersion curve is being matched by the old and the new models).

Conclusions

The SASW method offers the potential of evaluating shear-wave slowness profiles quickly and at relatively small cost. The comparison of slowness profiles from downhole seismic and SASW testing at 10 sites is generally good. This study demonstrates that in many situations the SASW method can provide slowness profiles suitable for site response predictions. Details of the layering are less important than the average depth dependence of the slowness. The differences in predicted ground-motion amplification between the slowness profiles from SASW and downhole testing are less than

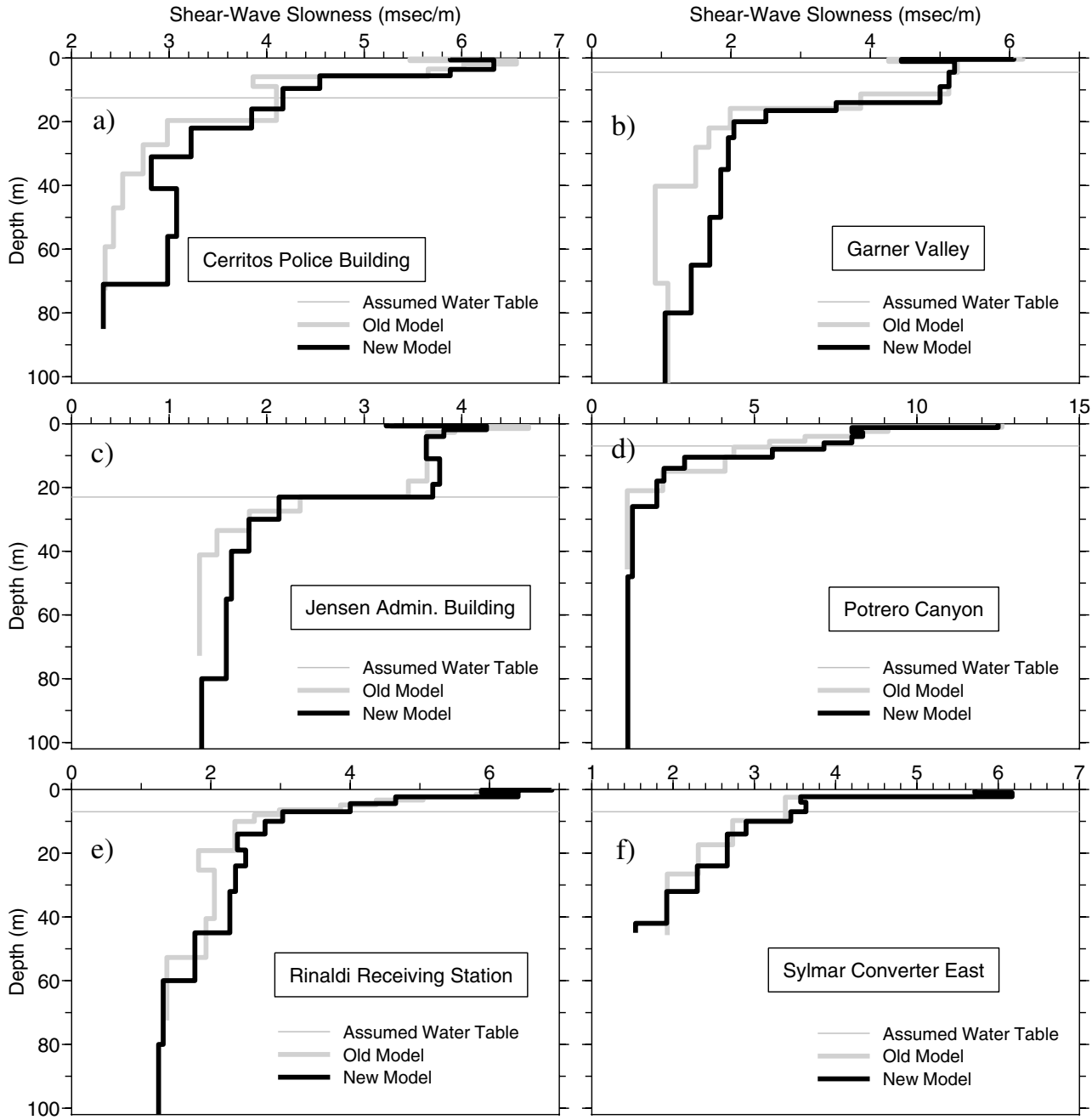

Figure 13. Comparison of shear-wave slownesses for model constructed assuming a constant Poisson's ratio (old model) and for model in which the water table was taken into account (see text) (new model). The assumed depth to the water table is shown by the horizontal line in each figure. (*Continued on next page.*)

about 15% for most frequencies, which is a minor difference.

SASW measurements are inherently different from borehole measurements since they average material properties over a much larger area. Lateral variations and inhomogeneities in the subsurface materials may cause differences in the slowness profiles from the two methods, with the interesting point being that both sets of measurements may correctly represent the material that has been sampled. Background information such as the approximate stratigraphy and depth to the groundwater table should be used in the SASW analysis for greater accuracy. At sites where there is a gradual increase in shear stiffness with depth, the fundamental-mode Rayleigh-wave dispersion model is a good approximation of the SASW experiment. At more complicated sites, surface-wave dispersion models that take into account receiver geometry, body-wave energy, and higher modes of Rayleigh-wave propagation may generally improve the solution.

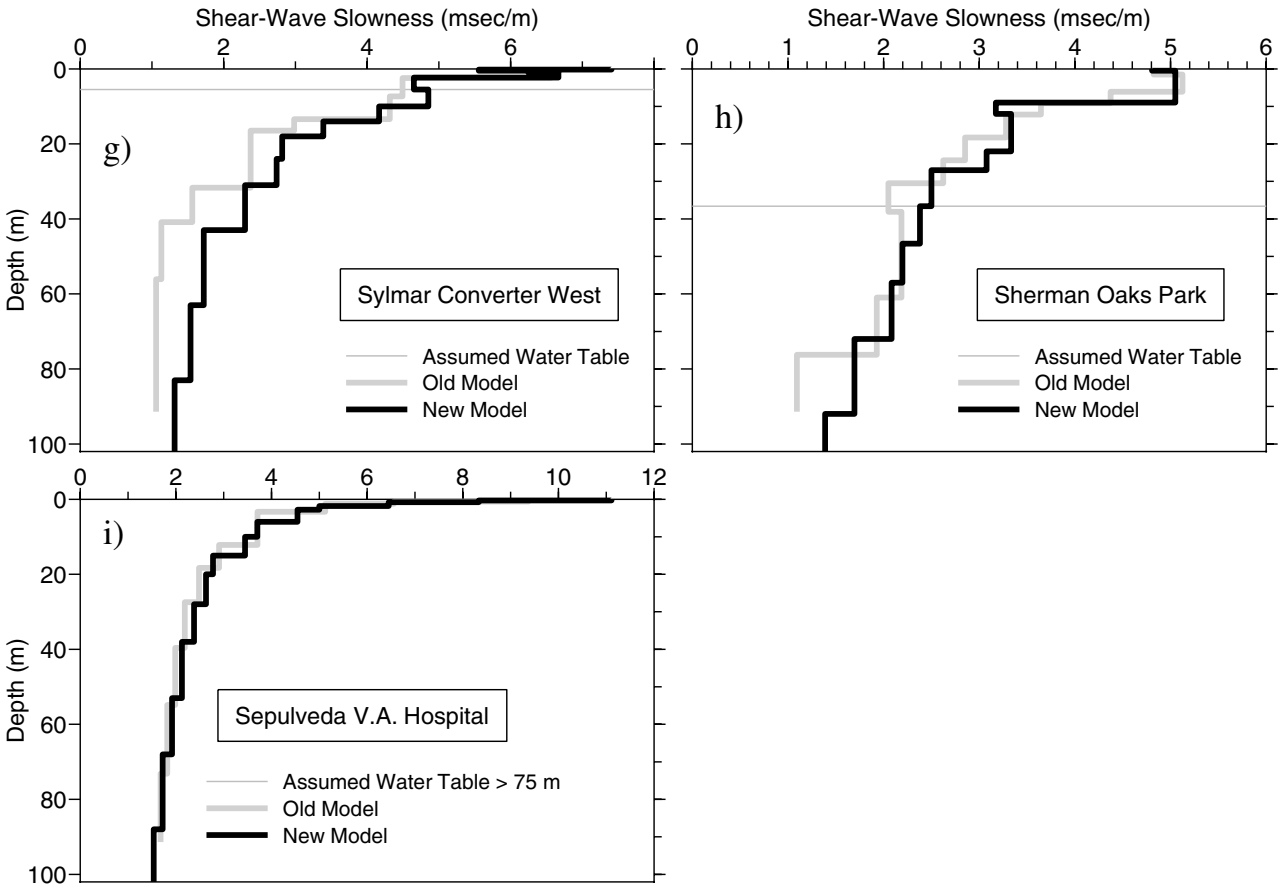

Figure 13. (*Continued*)

Acknowledgments

We thank numerous individuals who made it possible to obtain the field measurements. This includes Craig Davis and Ron Tognazzini of the Los Angeles Department of Water and Power (LADWP) for access to stations JMB, RIN, SCE, and SCW; University of Texas students Brent Rosenblad and James Bay, who oversaw collection of the field data and assisted in initial SASW data reduction; Jamie Steidl for information and access to the GV site; the ROSRINE group and Rob Stellar in particular for the PS log data and interpretations; Jeff Owen of LADWP for onsite guidance at RIN, SCE, and SCW; SECO for a great vibroseis crew; and the many unnamed property owners and managers for permission to conduct the surveys on their land. We'd also like to thank Jim Gibbs, Rob Kayen, and Glenn Rix for reviews and Bob Simons of Cohort Software for help with the software (CoPlot) used to produce the figures. This work was partially supported by Grant No. 1434-HQ-97-03060 from the U.S. Geological Survey.

References

Boore, D. M. (2003). Prediction of ground motion using the stochastic method, *Pure Appl. Geophy.* **160** (in press).

Boore, D. M., and L. T. Brown (1998a). Comparing shear-wave velocity profiles from inversion of surface-wave phase velocities with downhole measurements: systematic differences between the CXW method and downhole measurements at six USC strong-motion sites, *Seism. Res. Lett.* **69,** 222–229.

Boore, D. M., and L. T. Brown (1998b). Erratum to "Comparing shear-wave velocity profiles from inversion of surface-wave phase velocities with downhole measurements: systematic differences between the CXW method and downhole measurements at six USC strong-motion sites," *Seism. Res. Lett.* **69,** 406.

Boore, D. M., and W. B. Joyner (1997). Site amplifications for generic rock sites, *Bull. Seism. Soc. Am.* **87,** 327–341.

Brown, L. T. (1998). Comparison of VS profiles from SASW and borehole measurements at strong motion sites in Southern California, M.S. Thesis, University of Texas at Austin.

Gibbs, J. F. (1989). Near-surface *P*- and *S*-wave velocities from borehole measurements near Lake Hemet, California, *U.S. Geol. Surv. Open-File Rept. 89-630.*

Gibbs, J. F., D. M. Boore, J. C. Tinsley, and C. S. Mueller (2001). Borehole P-and S-wave velocity at thirteen stations in southern California, *U.S. Geol. Surv. Open-File Rept. OF 01-506*, 117 pp.

Gibbs, J. F., J. C. Tinsley, D. M. Boore, and W. B. Joyner (1999). Seismic velocities and geological conditions at twelve sites subjected to strong ground motion in the 1994 Northridge, California, earthquake: a revision of OFR 96-740, *U.S. Geol. Surv. Open-File Rept. 99-446*, 142 pp.

Gibbs, J. F., J. C. Tinsley, D. M. Boore, and W. B. Joyner (2000). Borehole velocity measurements and geological conditions at thirteen sites in the Los Angeles, California region, *U.S. Geol. Surv. Open-File Rept. OF 00-470*, 118 pp.

Horike, M. (1985). Inversion of phase velocity of long-period microtremor

to the S-wave-velocity structure down to the basement in urbanized areas, *J. Phys. Earth* **33,** 59–96.

Joh, S.-H. (1992). *User's Guide to WinSASW: Data Reduction and Analysis Program for Spectral Analysis of Surface Waves (SASW)*, University of Texas at Austin, 51 pp.

Joh, S.-H. (1997). Advances in interpretation and analysis techniques for spectral-analysis-of-surface-waves (SASW) measurements, Ph.D. Dissertation, University of Texas at Austin.

Nazarian, S., and K. H. Stokoe II (1984). In situ shear wave velocities from Spectral Analysis of Surface Waves, in *Proceedings of the Eighth World Conference on Earthquake Engineering*, Prentice-Hall, Inc., Englewood Cliffs, New Jersey, Vol. III, 31–38.

Nigbor, R. L., and T. Imai (1994). The suspension P-S velocity logging method, in *Geophysical Characterization of Sites, Technical Committee for XIII ICSMFE*, A. A. Balkema, Rotterdam, The Netherlands, 57–61.

Steidl, J. H., R. J. Archuleta, A. G. Tumarkin, L. F. Bonilla, and J. C. Gariel (1998). Observations and modeling of ground motion and pore pressure at the Garner Valley, California, test site, in *The Effects of Surface Geology on Seismic Motion* (K. Irikura, K. Kudo, H. Okada, and T. Sasatani, Eds.), A. A. Balkema, Rotterdam, The Netherlands, Vol. 1, 225–232.

Stokoe, K. H. II, G. L. Rix, and S. Nazarian (1989). In situ seismic testing with surface waves, in *Proceedings of the Twelfth International Conference on Soil Mechanics and Foundation Engineering*, Rio de Janeiro, Brazil, Vol. 1, 330–334.

Stokoe, K. H., II, S. G. Wright, J. A. Bay, and J. A. Roesset (1994). Characterization of geotechnical sites by SASW method, in *Geophysical Characterization of Sites, Technical Committee for XIII ICSMFE*, A. A. Balkema, Rotterdam, The Netherlands, 785–816.

Wills, C. J., M. Petersen, W. A. Bryant, M. Reichle, G. J. Saucedo, S. Tan, G. Taylor, and J. Treiman (2000). A site-conditions map for California based on geology and shear-wave velocity, *Bull. Seism. Soc. Am.* **90,** S187–S208.

Zywicki, D. J. (1999). Advanced signal processing methods applied to engineering analysis of seismic surface waves, Ph.D. Dissertation, Department of Civil Engineering, Georgia Institute of Technology.

Appendix A

Figures in Terms of Velocity Rather than Slowness

Presented here are the equivalents of Figures 6, 8, 11, and 13, but using velocity rather than slowness for the abscissa.

U.S. Geological Survey
345 Middlefield Rd., MS 977
Menlo Park, California 94025
boore@usgs.gov
(D.M.B., L.T.B.)

Department of Civil Engineering
Ernest Cockrell Jr. Bldg. 9.227
University of Texas at Austin
Austin, Texas 78712
k.stokoe@mail.utexas.edu
(L.T.B., K.H.S.)

Manuscript received 18 January 2002.

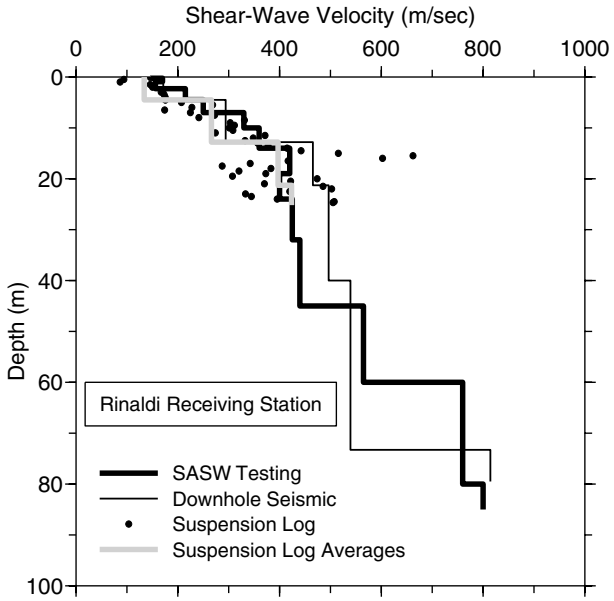

Figure A1. Repeat of Figure 6, in terms of velocity rather than slowness.

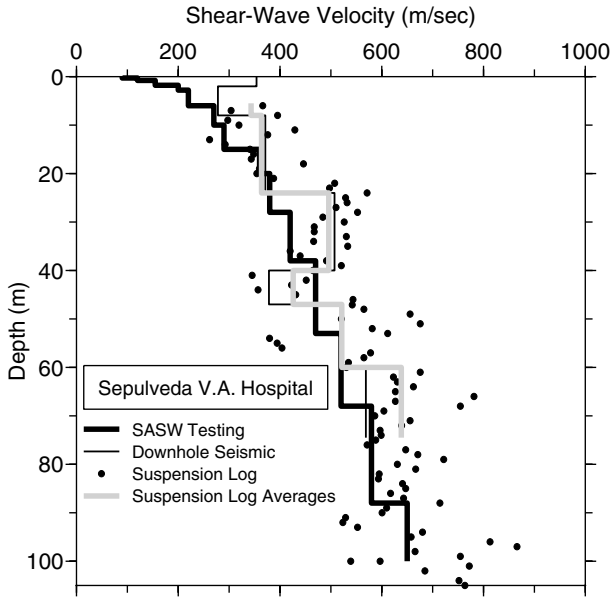

Figure A2. Repeat of Figure 8, in terms of velocity rather than slowness.

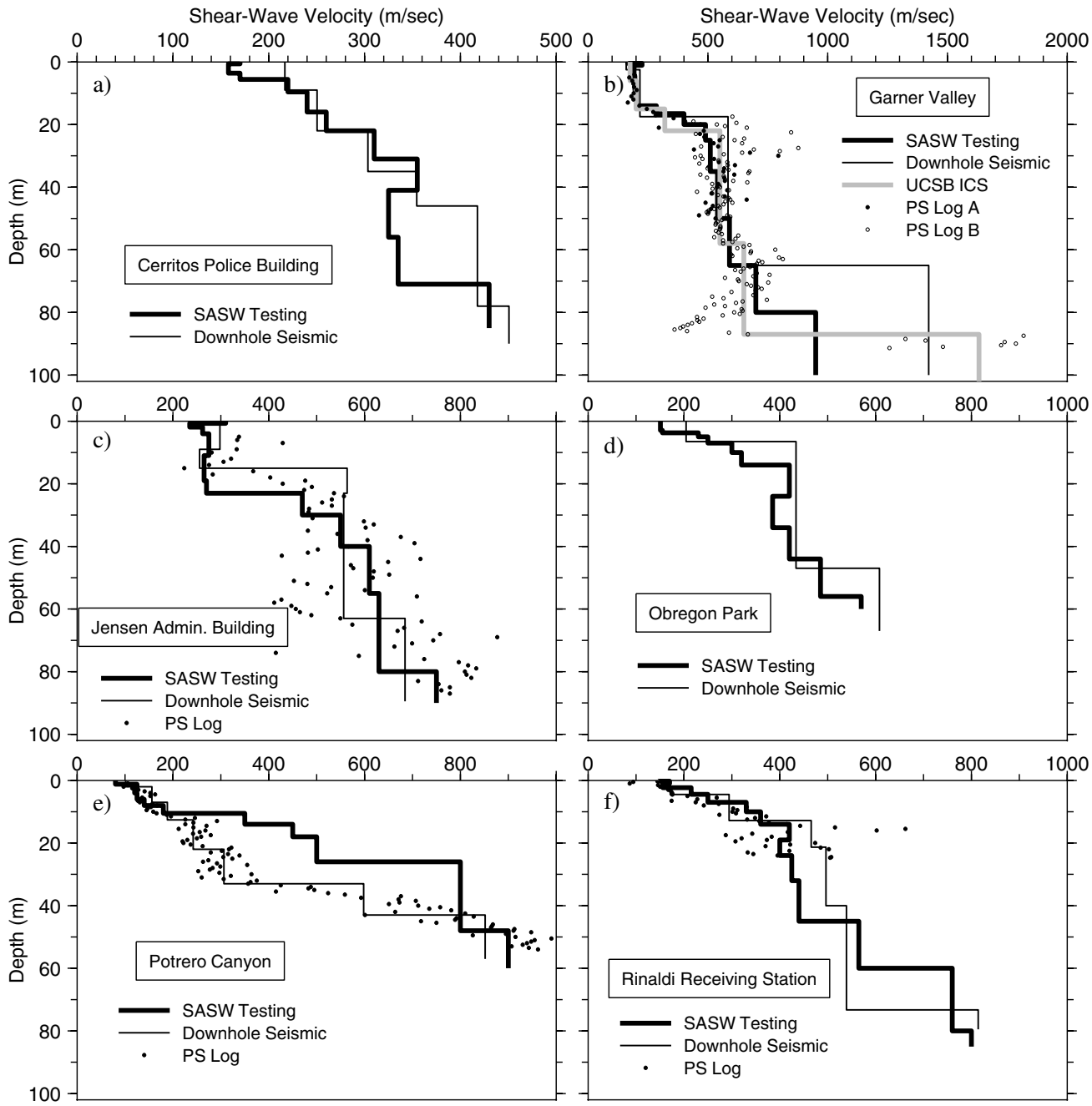

Figure A3. Repeat of Figure 11, in terms of velocity rather than slowness.

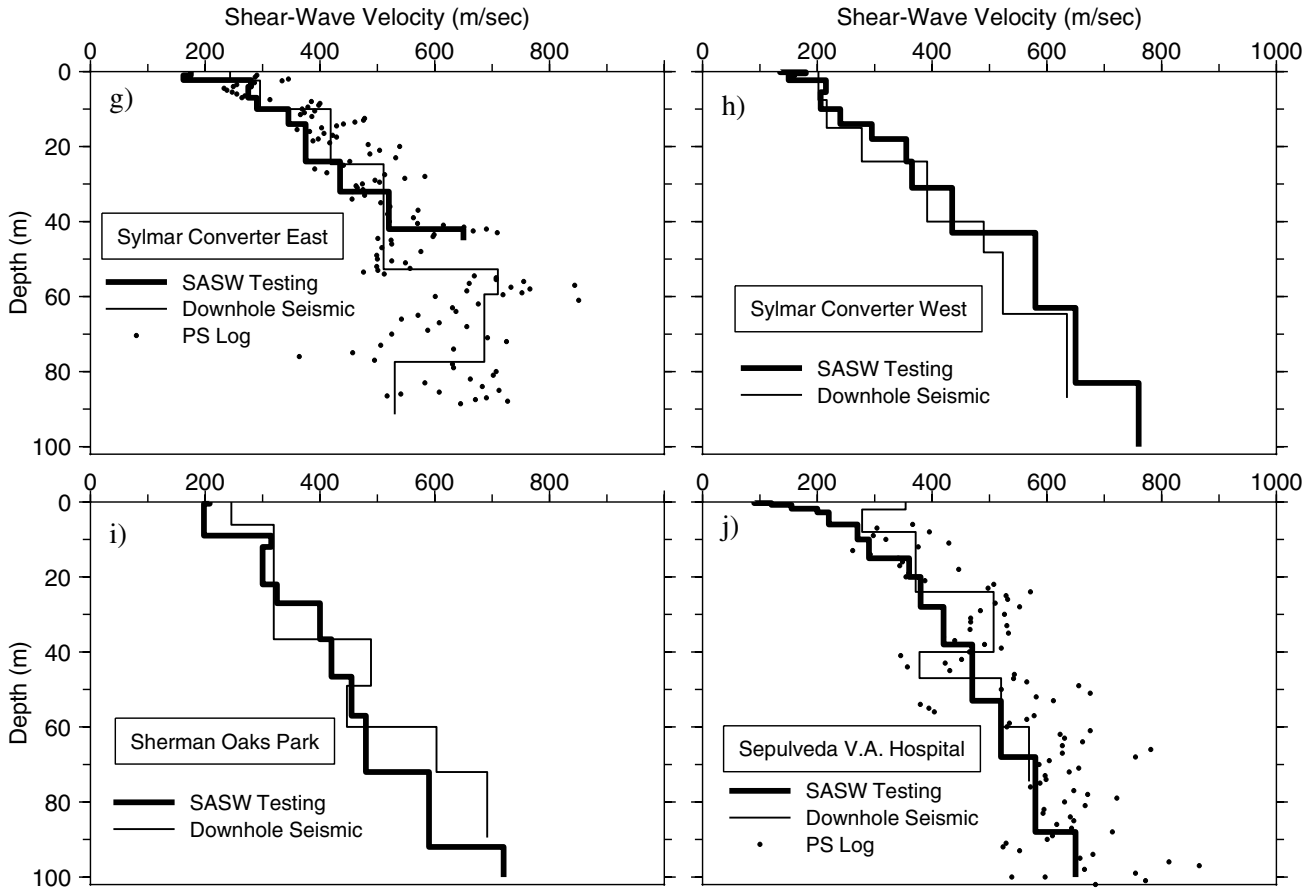

Figure A3. (*Continued*)

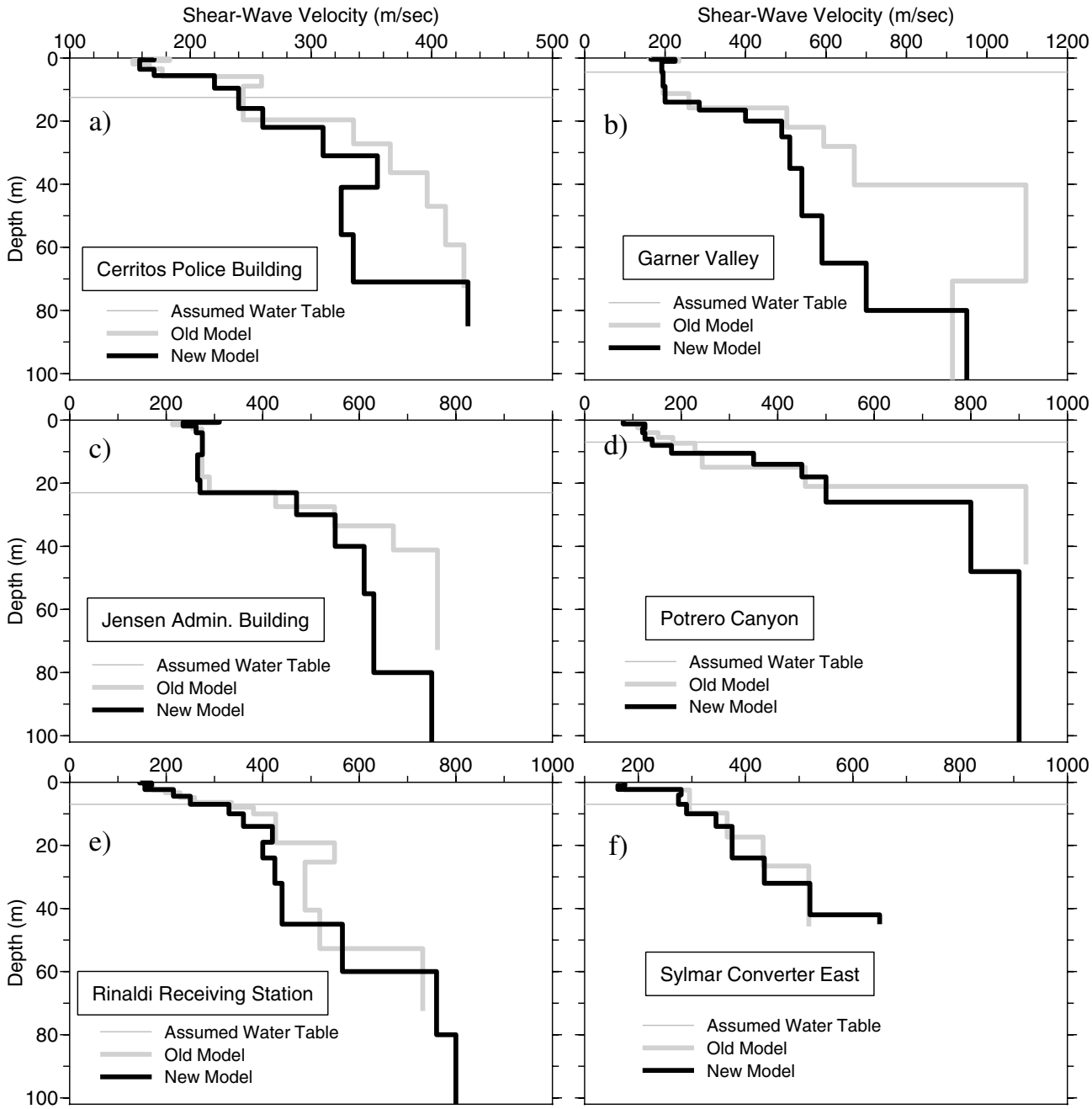

Figure A4. Repeat of Figure 13, in terms of velocity rather than slowness.

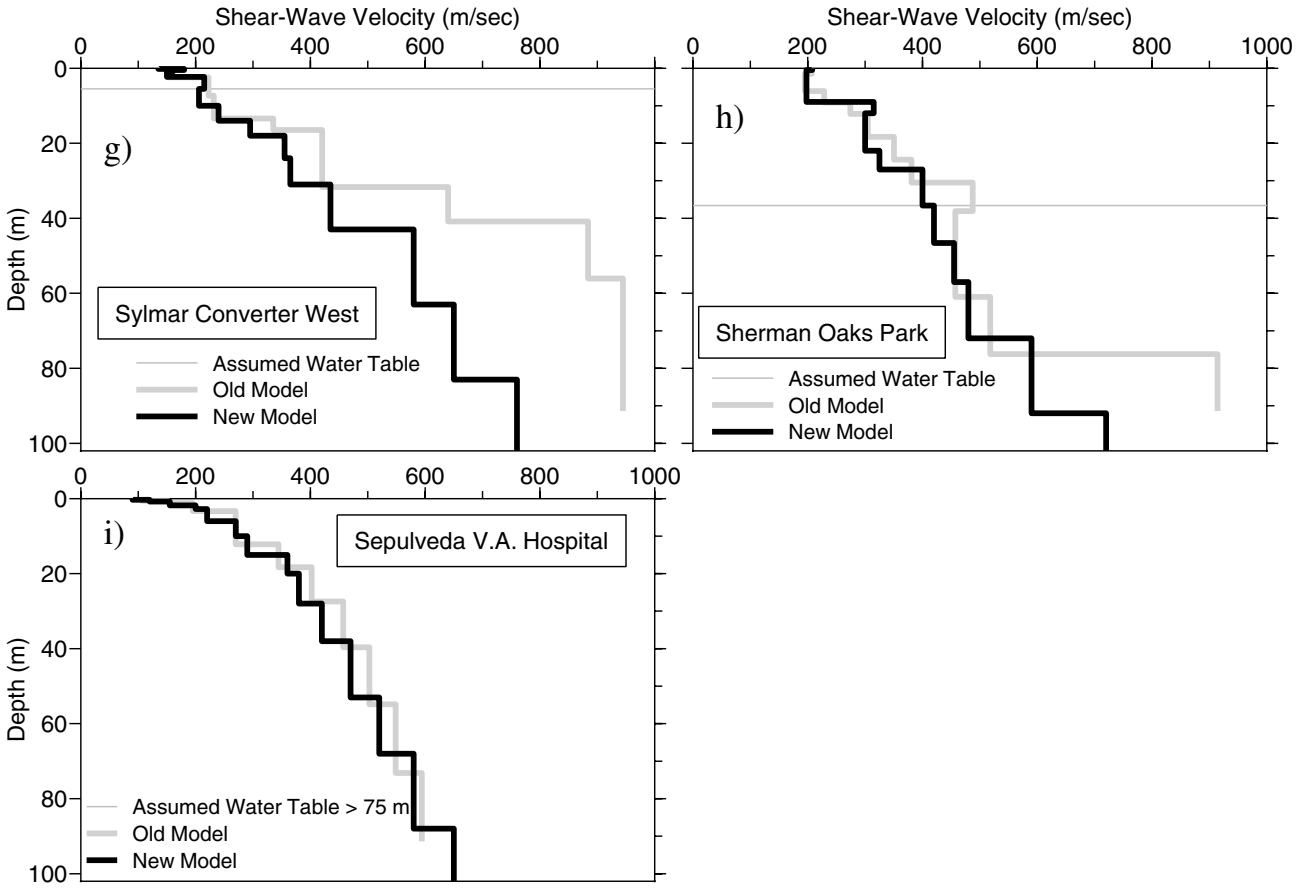

Figure A4. (*Continued*)